Pressure induced phase transitions in GeTe - rich Ge-Sb-Te alloys across the rhombohedral to cubic transitions.

Milos Krbal,[*,†] Jaroslav Bartak,[‡] Jakub Kolar,[¶] Anastasiia Prytuliak,[§] Alexander V. Kolobov,[‖] Paul Fons,[‖] Lucile Bezacier,[⊥] Michael Hanfland,[⊥] and Junji Tominaga[‖]

Faculty of Chemical Technology, Center of Materials and Nanotechnologies (CEMNAT), University of Pardubice, Legions Square 565, 530 02 Pardubice, Czech Republic, Faculty of Chemical Technology, Department of Physical Chemistry, University of Pardubice, Studentska 573, 53210 Pardubice, Czech Republic, Faculty of Chemical Technology, Department of General and Inorganic Chemistry,University of Pardubice, Studentska 573, 53210 Pardubice, Czech Republic, European Space Agency, Keperlaan 1, 2201 AZ Noordwijk, The Netherlands, Nanoelectronics Research Institute, National Institute of Advanced Industrial Science and Technology 1-1-1 Higashi, Tsukuba 305-8562, Ibaraki, Japan, and European Synchrotron Radiation Facility (ESRF), 6 rue Jules Horowitz, Boîte Postale 220, F38043, Grenoble, France

E-mail: milos.krbal@upce.cz

Abstract

We demonstrate that pressure induced amorphization in Ge-Sb-Te alloys across the ferroelectric-paraelectric transition can be represented as a mixture of coherently distorted rhombohedral $Ge_8Sb_2Te_{11}$ and randomly distorted cubic $Ge_4Sb_2Te_7$ and high temperature $Ge_8Sb_2Te_{11}$ phases. While coherent distortion in $Ge_8Sb_2Te_{11}$ does not prevent the crystalline state from collapsing into its amorphous counterpart in a similar manner to pure GeTe, the pressure-amorphized $Ge_8Sb_2Te_{11}$ phase begins to revert to the crystalline cubic phase at about 9 GPa in contrast to $Ge_4Sb_2Te_7$ which remains amorphous under ambient conditions when gradually decompressed from 40 GPa. Moreover, experimentally, it was observed that pressure induced amorphization in $Ge_8Sb_2Te_{11}$ is a temperature dependent process. $Ge_8Sb_2Te_{11}$ transforms into the amorphous phase at about 27.5 and 25.2 GPa at room temperature and 408 K, respectively and completely amorphizes at 32 GPa at 408 K while some crystalline texture could be seen until 38 GPa (the last measurement point) at room temperature. In order to understand the origins of the temperature dependence of the pressure induced amorphization process, DFT calculations were carried out for compositions along the $(GeTe)_x - (Sb_2Te_3)_{1-x}$ tie line under large hydrostatic pressures. The calculated results agreed well with the experimental data.

Introduction

Tellurium-based alloys, especially those alloys lying along the quasibinary $(GeTe)_x - (Sb_2Te_3)_{1-x}$ tie-line and Sb-rich Sb-Te, posses the unique ability to transform quickly and reversibly between amorphous and crystalline phases.[1–6] The phase transition is accompanied by abrupt and significant changes in optical properties as well as changes in resistivity of a few orders of magnitude that can serve to encode information. This phenomenon has been commercialized in data storage applications such as DVD and Blu-ray optical memory as well as non-volatile phase change electrical memory. In principle, data is recorded by means of a short intense laser or electrical pulse with a duration of tens of nanoseconds which adds sufficient energy to melt or to disorder the crystalline phase followed by a subsequent rapid quench to form an amorphous bit. Conversely,

erasure of a recorded mark is achieved by applying a less intense, longer duration pulse (hundreds of nanoseconds) which heats the amorphous region above the crystallization temperature and thus reverts the material into the crystalline state.

The recorded bits in both optical and electronic data storages are amorphous (or crystalline) areas embedded in a crystalline (or amorphous) matrix. Since the densities of the two phases are different, momentarily stresses are inevitably generated in the recorded bits and at interfaces and are likely to play an important role in device performance. In addition, encapsulation materials such as TiN may exert additional compressive stress with values of 240 MPa being reported.[7] Recently, it has been reported that interfacial strain engineered $(GeTe)_x - (Sb_2Te_3)_{1-x}$ superlattices can reduce the switching energy of the structure, decrease the switching time and voltage of phase change memory cells.[8,9] External compressive or tensile stresses can be also generated by uniaxial stress or the bending of the active layer leading to effects on crystallization.[10] The investigation of phase transitions under pressure is of both fundamental and practical interest. Applied pressure can reversibly or irreversibly affect the structure of the crystalline surroundings of the amorphous bit as well as the stability of recorded information. Stress may also reduce the band gap, increase the conductivity by several orders of magnitude,[11] make recrystallization more likely[12] and decrease the melting point.[13]

Recently, it was demonstrated that cubic $Ge_2Sb_2Te_5$ and $Ge_1Sb_2Te_4$ (low temperature modification) with randomly localized vacancies can be rendered amorphous under hydrostatic pressures above 16 GPa, while trigonal $Ge_2Sb_2Te_5$ (high temperature modification) cannot due to vacancy ordering in the van der Waals gap.[14,15] Additional studies performed in[16] also confirmed the important role of vacancies on pressure induced amorphization (PIA). Analogously, the end-points of the $(GeTe)_x - (Sb_2Te_3)_{1-x}$ tie-line such as trigonal Sb-Te based alloys do not amorphize for the same reason while the rhombohedral GeTe phase does not collapse to the amorphous state because of the absence of vacancies when compressed.[17–20] At ambient conditions, pure crystalline GeTe exists in the rhombohedral phase, where the six Ge-Te bonds are split into three shorter and three longer bonds. When GeTe is mixed with Sb_2Te_3 , the rhombohedral structure is preserved until the

concentration of Sb_2Te_3 exceeds 14 % upon which the rock-salt-like cubic phase (on average) can be observed[21] via Bragg diffraction while the preservation of the 3+3 bond splitting was revealed by EXAFS.[23] In addition to the crystallographic changes, the presence of Sb_2Te_3 in the GeTe host matrix leads to the formation of structural vacancies which increase static disorder in the crystalline phase and at the same time creates room for triggering pressure induced amorphization.[24]

For instance, in Blu-Ray disk technology, GeTe-rich Ge-Sb-Te, namely $Ge_8Sb_2Te_{11}$ exists in the rhombohedral phase for concentrations of Sb_2Te_3 of about 11 % corresponding to a concentration of about 9 % vacancies in the cation sublattice. The composition is also located near the rhombohedral-to-cubic transition (see Fig. 1) as measured using Bragg diffraction.[21] When the temperature rises above 363 K, Bragg diffraction measurements indicate the rhombohedral phase transforms into the high temperature cubic phase. It is important to stress that vacancies are assumed to be randomly localized in both phases. Recently, it was concluded that this transformation is an order-disorder transition rather than displacive with the apparent rock-salt structure resulting from the local rhombohedral distortion changing from coherent (Ge atoms are distorted in one direction) below the Curie point to stochastic (Ge atoms are randomly distorted) above the Curie point.[22,23] Since coherently distorted rhombohedral GeTe has less than a percent of intrinsic vacancies in the Ge sublattice,[25] it does not undergo PIA. It is speculated that the coherent distortion in rhombohedral $Ge_8Sb_2Te_{11}$ may hamper or at least strongly influence the PIA phenomenon in contrast to the cubic high temperature modification. It is important to stress that the concentration of vacancies in the low and high temperature modifications of $Ge_8Sb_2Te_{11}$ should be similar and thus only the initial structure may play a role in PIA.

In order to better understand pressure-induced phase transitions around the ferroelectric-paraelectric transition (i.e. between the coherently distorted rhombohedral and the randomly distorted cubic phases), and in particular the crystal-to-amorphous transition in GeTe-rich Ge-Sb-Te alloys, we investigated high-pressure phase transitions in rhombohedral $Ge_8Sb_2Te_{11}$ (11 % of Sb_2Te_3) and cubic $Ge_4Sb_2Te_7$ (containing 20 % of Sb_2Te_3 which is close to the rhombohedral-to-cubic transition from the other end of the tie-line) at room temperature to determine whether the admixture of

14% of Sb_2Te_3 in GeTe could serve as a trigger for PIA along the $(GeTe)_x - (Sb_2Te_3)_{1-x}$ tie-line. Since $Ge_8Sb_2Te_{11}$ undergoes a rhombohedral-to-cubic transition at about 363 K, we also compressed cubic $Ge_8Sb_2Te_{11}$ at 408 K to study the role of the initial state on PIA (see Fig.1) since the concentration of vacancies is the same for both phases of $Ge_8Sb_2Te_{11}$.

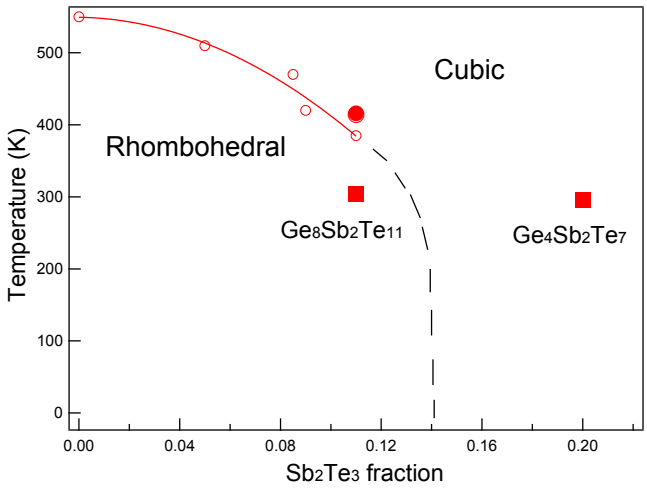

Figure 1: (Color online) Phase diagram of the rhombohedral and cubic phases and their dependence on temperature and Sb_2Te_3 fraction. The red closed marks represent the Ge-Sb-Te compositions along the rhombohedral-to-cubic transition that were studied in the current experiment and open circles show data reported in.[21]

Experimental details and Simulations

$Ge_8Sb_2Te_{11}$ and $Ge_4Sb_2Te_7$ (cubic phase) samples were deposited on silicon substrates using magnetron sputtering and flash evaporation. The thickness of the films was about 500 nm. The samples were then subsequently crystallized at 503 K for one hour in an Argon ambient to prevent sample oxidation.

A series of diffraction measurements were then carried out from ambient pressure to 40 GPa in steps of 2 GPa at room temperature and 408 K at beam line ID09A at the ESRF (Grenoble, France). The samples consisted of $Ge_8Sb_2Te_{11}$ and $Ge_4Sb_2Te_7$ placed in the gasket hole between the anvils of a diamond anvil cell. Helium and Neon gas were used as pressure transmitting media to ensure the best possible hydrostatic conditions. Photoluminescence from a ruby included in the

gasket hole was used as a pressure marker to determine the pressure in the cell. Debye-Scherrer diffraction images were collected with a monochromatic beam ($\lambda = 0.415$ Å) focused to ca. 20 $\times$ 20 μm using a a MAR555 flat panel detector. The pressure was increased or decreased in steps of ca. 2 GPa and the system was allowed to equilibrate for 5 to 10 minutes at each pressure point which is a time typically used in similar experiments. The acquisition time was typically 2 - 10 seconds. Rietveld refinement was used to obtain accurate lattice parameters for the measured samples using the FullProf package.

Density functional calculations were carried out using the plane-wave code CASTEP.[26] Ultra-soft pseudopotentials were used for germanium, antimony, and tellurium atoms. The germanium, antimony, and tellurium pseudopotentials included the germanium $4s^2$ $4p^2$, antimony $5s^2$ $5p^3$, and tellurium $5s^2$ $5p^4$ states as valence electrons, respectively. The DFT exchange correlation contribution was evaluated using the local density approximation (LDA) for the exchange potential. The LDA term was formulated from the numerical results of Ceperley and Alder[27] as parameterized by Perdew and Zunger.[28]The charge density was calculated with a plane-wave cutoff of 220 eV and a 2 $\times$ 2 $\times$ 2 Monkhorst-Pack grid. In our DFT calculations, a calculation cell containing 64 atomic positions (atoms and vacancies) was compressed under NPT conditions in pressure steps of 2 GPa. Each pressure step was relaxed for 15 ps with a time steps of 3 fs.

Results and discussion

In order to investigate the role of the initial structure across the ferroelectric-paraelectric transition in Ge-Sb-Te alloys on PIA, we performed a high pressure study on the high temperature forms of $Ge_8Sb_2Te_{11}$ and $Ge_4Sb_2Te_7$ which possess a rock-salt like structure and the low temperature modification of $Ge_8Sb_2Te_{11}$ which forms in a rhombohedrally distorted phase.

The behavior of $Ge_4Sb_2Te_7$ upon compression and decompression is shown in Fig. 2. The initial structure belongs to $Fm\bar{3}m$ space group with the lattice parameter a = 6.007 Å When compressed, the collapse of the cubic phase appears at 22.6 GPa and the amorphization process con-

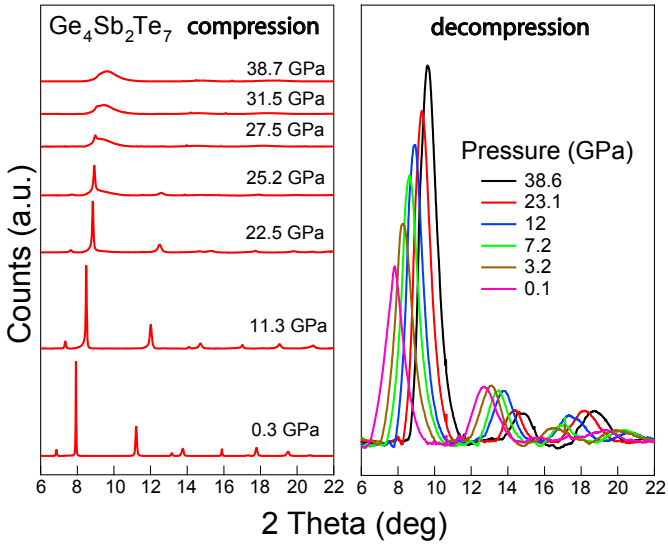

Figure 2: (Color online) The evolution of the synchrotron based X-ray diffraction patterns of $Ge_4Sb_2Te_7$ upon compression (left) and decompression (right).

tinues until the crystalline phase totally disappears at about 30 GPa. The phase transition sequence in $Ge_4Sb_2Te_7$ resembles the high pressure phase transitions occurring in cubic $Ge_2Sb_2Te_5$ and $Ge_1Sb_2Te_4$ in which amorphization starts at significantly lower pressures 15 [14,15,29] and 12 GPa, [16] respectively with samples becoming totally disordered at 25 GPa and finally recrystallizing at 34 GPa into the body-centered-cubic (BCC) phase. In contrast to $Ge_2Sb_2Te_5$ ($Ge_1Sb_2Te_4$), pressure amorphized $Ge_4Sb_2Te_7$ does not transform into the BCC structure until 40 GPa, which was the highest pressure attained in the current experiment.

Upon decompression, the amorphous state is preserved until ambient pressure. From Fig. 2 (right panel) it can be seen that the intensity of the main broad peak (from 6 to 10 deg) gradually diminishes with decreasing pressure. This dependence may indicate a change in coordination of the underlying structural units, from BCC like units (coordination number 8) to tetrahedrons (coordination number 4) and pyramids (coordination number 3) when the pressure is gradually released. Such an concept is in good agreement with in silico simulations of the PIA phenomenon in $Ge_2Sb_2Te_5$ [30] when the so-called "t-amorphous" state (where t-represents a trigonal texture in the amorphous state) transforms at 30GPa to a state equivalent to the so-called "melt quenched" phase at ambient pressure. The same conclusion was obtained from the numerical study of an

atomistic model which exhibited a one-step crystal-to-amorphous transition upon decompression demonstrating that the pressure - induced amorphous phase cannot be distinguished from that obtained by quenching from the melt.[31]

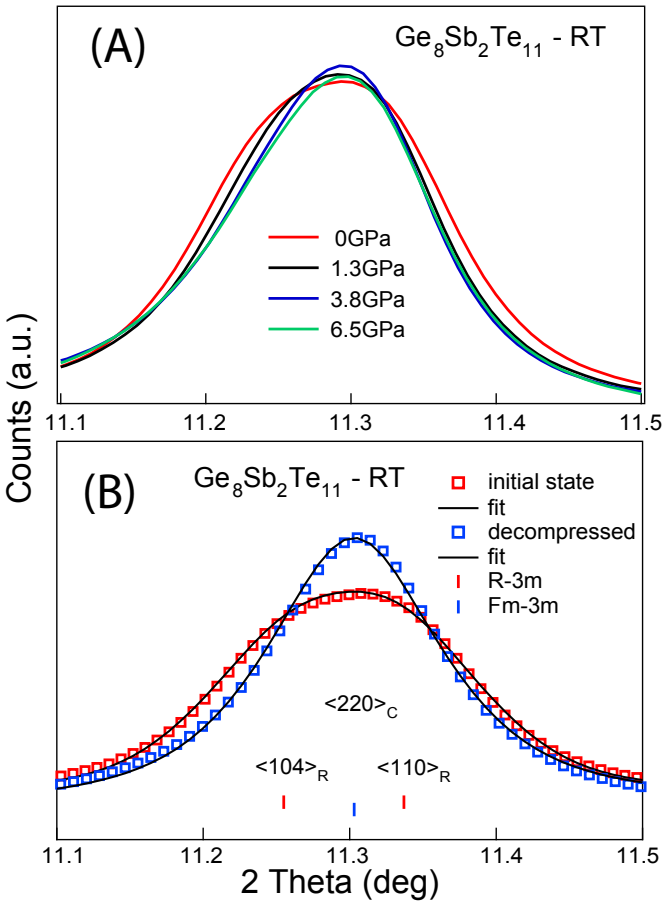

Figure 3: (Color online) The ferroelectric to paraelectric transition observed in the low-temperature phase of $Ge_8Sb_2Te_{11}$ via Bragg diffraction: A) under compression (upper figure) - in the figure, the diffraction peaks were aligned to the same two theta value in order to emphasize the rhombohedral to cubic transition B) before compression and after decompression (bottom figure). The most conspicuous change in the diffraction pattern due to the transition can be characterized by diffraction peaks $\langle 104 \rangle_R$ and $\langle \bar{1}10 \rangle_R$ for the initial rhombohedral phase and $\langle 220 \rangle_C$ for the decompressed cubic phase. The experimental data were collected at the wavelength $\lambda = 0.415$ Å.

The low temperature $Ge_8Sb_2Te_{11}$ phase crystallizes into the rhombohedral phase with the lattice parameters a = 4.201 Å and c = 10.413 Å in the hexagonal setting. From Fig. 3 it is obvious that positions of the diffraction peaks $\langle 104 \rangle_R$ and $\langle \bar{1}10 \rangle_R$ which characterize the rhombohedral structure are close to each other. In comparison with the low temperature modification of GeTe[32]

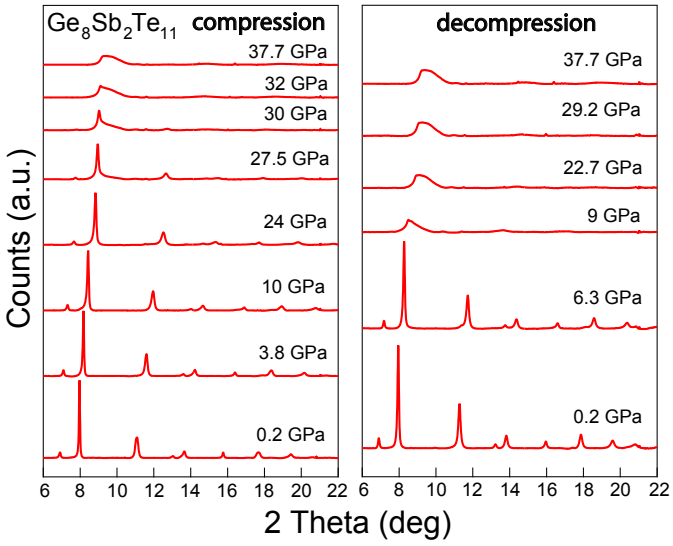

Figure 4: (Color online) The evolution of the synchrotron based X-ray diffraction patterns of $Ge_8Sb_2Te_{11}$ upon compression (figures on the left) and decompression (figures on the right).

this rhombohedral peak splitting is very small. There are at least two factors that may explain this observation. First, it has been suggested that the three Ge(Sb) atoms connected with longer bonds to Te atoms located near the vacancy move from the $\langle 111 \rangle$ to the $\langle \bar{1}\bar{1}\bar{1} \rangle$ crystallographic directions resulting in an increase in the static disorder of the structure.[20] As a consequence, the neighboring Te atoms locally reorder as well which is accompanied with a shift in the cell angle on a global scale from the rhombohedral-to-cubic.[33] However, the second factor may be simply experimental. In a previous work,[21] a larger peak splitting of the $\langle 104 \rangle_R$ and $\langle \bar{1}10 \rangle_R$ peaks was observed than in the current experiment. Deposition and subsequent annealing conditions might also thus play an appreciable role on the crystallographic parameters of $Ge_8Sb_2Te_{11}$.

Upon compression (see panel a in Fig. 3 and Fig. 4), the $Ge_8Sb_2Te_{11}$ rhombohedral structure transforms to the cubic phase at about 3.8 GPa which is a pressure comparable to that for which the rhombohedral-to-cubic transition appears in pure GeTe.[34,35] The detailed rhombohedral-to-cubic transition is shown in Fig. 3 (panel a) representing the zoomed-in XRD spectra emphasizing the characteristic diffraction peaks. Note, that the rhombohedral-to-cubic phase transition was determined by Rietveld refinement of XRD patterns using the FullProf package. Under further compression, the rock-salt like cubic phase remains until 27.5 GPa marking the onset of PIA with

completion of the amorphization process occurring at about 35 GPa. However as can be seen from Fig. 4 and Fig. 5 (panel a), a cubic texture remains even at 38 GPa. It is speculated that the cubic texture is formed in $Ge_8Sb_2Te_{11}$ when Ge (and/or Sb) are coherently displaced in a single crystallographic direction ($\langle 111 \rangle$ being typical for the rhombohedral phase) upon exposure to large hydrostatic pressure. Due to a lack of room it could be difficult for atoms to deviate from their crystal positions and thus the existence of an such ordered area may suppress PIA. These inclusions could be more resistant to breakup under significant stress than regions of $Ge_8Sb_2Te_{11}$ with structural vacancies. In general, vacancies break the coherency of distortions and promote nanophase separation that often serves as a driving force for PIA.[36] Similarly to $Ge_4Sb_2Te_7$, $Ge_8Sb_2Te_{11}$ does not transform to the BCC phase until 40 GPa. Surprisingly, upon decompression, the amorphous phase reverts into the cubic phase between 9 to 6 GPa and remains stable until return to the ambient environment.

The high temperature modification of $Ge_8Sb_2Te_{11}$ forms in the cubic structure (space group $Fm\bar{3}m$) with lattice parameter a = 5.983 Å. Under elevated pressure, the cubic phase commences to disorder at 25.2 GPa which is approximately 2 GPa lower than in the case of its low temperature modification (see Fig. 5 panel b). In addition, the material becomes fully amorphous at about 32 GPa without any sign of a crystalline texture which might have resulted from the distortion changing from coherent below the Curie point to stochastic above the Curie point (an order-disorder transition).[23] This result indicates that PIA in $Ge_8Sb_2Te_{11}$ may be thermally activated and it is speculated that thermal atomic disorder may reduce the pressure at which crystalline Ge-Sb-Te transforms into the amorphous state. Upon decompression, the cubic phase returned in the same pressure range as the RT modification.

It is interesting to note the effect of temperature on PIA in $Ge_8Sb_2Te_{11}$ while a previous study on $Ge_2Sb_2Te_5$[29] demonstrated that PIA is thermally insensitive. In general, the crystal-to-amorphous transformation is always triggered by mechanical instabilities. Temperature can give rise to a transition which occurs before the mechanical stability limit is reached due to the presence of a thermally activated barrier.[31] In order to explore and verify the thermal component of PIA

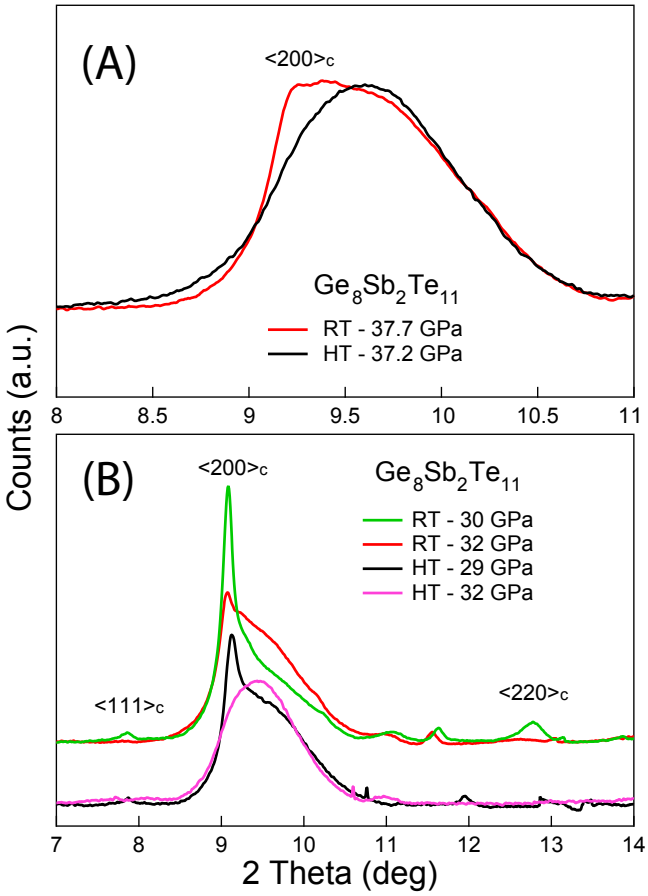

Figure 5: (Color online) Panel A clearly shows a signature of the remaining $\langle 200 \rangle_C$ peak in $Ge_8Sb_2Te_{11}$ compressed to $\approx$ 38 GPa at room temperature. Figure B demonstrates the experimentally observed thermal effect on the pressure induced amorphisation in $Ge_8Sb_2Te_{11}$ measured at room temperature (RT) and 135 °C (HT).

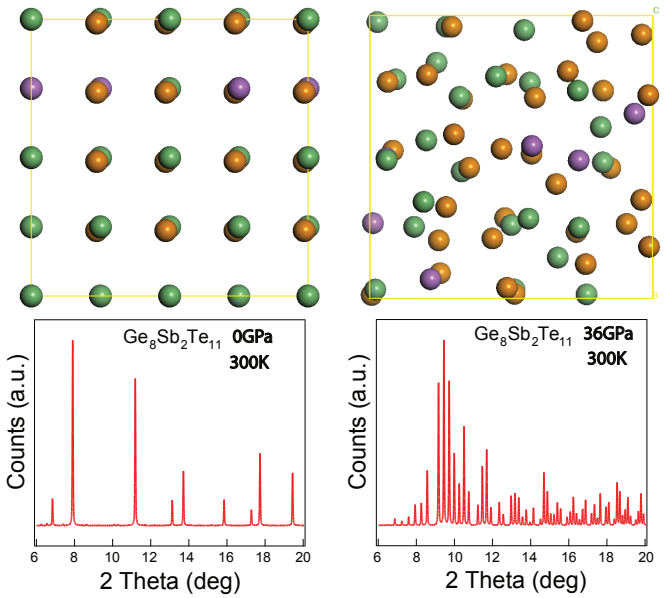

Figure 6: (Color online)The cubic and pressure induced amorphous phases (top) and their corresponding diffraction patterns (bottom) for $Ge_8Sb_2Te_{11}$ at 0 GPa (left panel) and compressed to 36 GPa (right panel) using DFT simulations at 300 K (Ge - green, Sb - violet, Te - gold).

along the $(GeTe)_x - (Sb_2Te_3)_{1-x}$ tie-line, we performed DFT calculations on $Ge_8Sb_2Te_{11}$, $Ge_4Sb_2Te_7$, $Ge_2Sb_2Te_5$, and $Ge_1Sb_2Te_4$ at 1, 50, 100, 200, 300, 400 and 500 K (see more in experimental details). In our simulations we compressed all structures incrementally until the PIA state was observed over a time period ranging from 8 to 10 ps to avoid introduction of a time dependence originating from the PIA simulation. We characterized a structure as being in the amorphous state when its calculated Bragg diffraction spectra changed from one characteristic of the $Fm\bar{3}m$ space group to a single broad peak (please, take in mind the enveloping curve), typical of the amorphous state as demonstrated in Fig. 6. Prior to further analysis, our model of pressure amorphized $Ge_2Sb_2Te_5$ generated at 26 GPa was compared with recently reported models containing more atoms. It was found that the total coordination numbers for Ge, Sb and Te using the cut off distance 3.1 A are 6.25, 6 and 4.29, respectively which are in concert with the work published by Sun et al.[30] Next, our model contains 17.5 % of Ge(Sb)-Ge(Sb) and 9.9 % of Te-Te wrong bonds which is in good agreement with values obtained by Cavarati et al.[24]

In Fig. 7 one can see a pressure-temperature plot of PIA in Ge-Sb-Te alloys constructed from the calculated values. First, we compared the calculated and experimentally obtained pressure

points at approximately 300 and 400 K for $Ge_2Sb_2Te_5$,[29] $Ge_4Sb_2Te_7$ and $Ge_8Sb_2Te_{11}$ when the structures became totally amorphous. We found that our models became completely disordered at the same pressure points as in our experiments which supports the relevance of the P-T plots for the following analysis although we are aware that the time scale of the DFT calculations and real experiments are different. Furthermore, it should be noted that the pressure-temperature dependence is exponential which suggests that PIA in Ge-Sb-Te alloys is thermally assisted. However, from Fig. 7 it can be discerned that the PIA is nearly thermally insensitive above 300 K for alloys containing a large number of vacancies (e.g. $Ge_2Sb_2Te_5$ and $Ge_1Sb_2Te_4$) which suggests that thermal effects can be suppressed in the presence of a large concentration of destabilization centers, e.g. vacancies. The difference in pressure for PIA between 300 K and 400 K is about 1 GPa which is in good agreement with the experimental observations for $Ge_2Sb_2Te_5$.[29] In contrast, there is still a conspicuous thermal influence in $Ge_8Sb_2Te_{11}$ above 300K which indicates that a structure with a low vacancy concentration needs to be supported by atomic thermal vibrations in order to reduce the pressure for which the crystal-to-amorphous transition occurs. This trend is also in agreement with experimental results. To understand the effects of pressure alone on PIA and thus to eliminate the thermal component, simulations were carried out at 1 K. Under these conditions, it was found that $Ge_2Sb_2Te_5$ amorphizes at about 56 GPa which is an excellent fit to the P-T curve for $Ge_2Sb_2Te_5$ while $Ge_8Sb_2Te_{11}$ does not convert to the amorphous phase until 100 GPa at 1K which is about 15 GPa higher pressure value than the predicted value from the pressure-temperature plot. Therefore it might be speculated that thermal disorder in rhombohedral $Ge_8Sb_2Te_{11}$ is prerequisite for the crystalline state to collapse into a disordered state under hydrostatic stress. Nonetheless, it is fair to point out that there is currently no cryogenic experimental data collected which could be compared with our simulations.

Last but not least, it is worth mentioning the influence of vacancy concentration on PIA. It was showed that PIA is indirectly related to the vacancy concentration at room temperature[16] which is consistent with our simulations. In addition, in Fig. 8 it can be seen that the concentration of structural vacancies affects exponentially the pressure points at which alloys along the

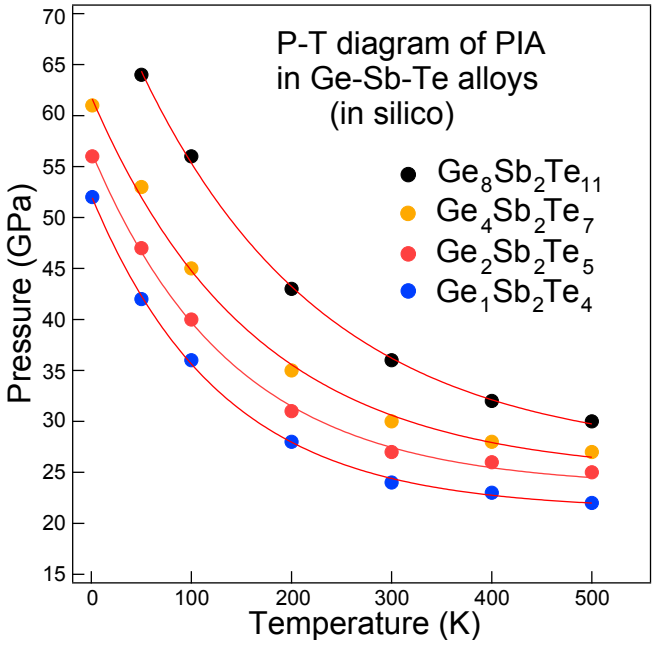

Figure 7: (Color online) In silico calculated Pressure-Temperature diagram of pressure induced amorphization in Ge-Sb-Te alloys. The calculated points represent the total amorphization of the crystalline Ge-Sb-Te phases at each temperature.

$(GeTe)_x - (Sb_2Te_3)_{1-x}$ quasi-binary tie-line become completely pressure amorphized. Experimentally, α-GeTe, the end point of the tie-line, undergoes only a crystal-to-crystal transitions to the final BCC phase which appears at about 46 GPa.[34] Under the assumption that 46 GPa is the maximum pressure at which PIA can be observed along $(GeTe)_x - (Sb_2Te_3)_{1-x}$, using Fig. 8, it can be predicted that $Ge_{22}Sb_2Te_{25}$ with about 4 % structural vacancies in the cation sublattice may constitute the border composition which might proceed only the crystal-to-crystal transition at 300 K.

Now we address the question of why $Ge_8Sb_2Te_{11}$ becomes crystalline when decompressed to about 9 GPa while $Ge_4Sb_2Te_7$ with a higher concentration of vacancies does not. We believe that the reason is twofold. On the one hand, through ab initio simulations, it was demonstrated that PIA starts when tellurium atoms sitting next to vacancies are squeezed into these vacant positions[24] which is also associated with the formation of homopolar bonds, in particular the Te-Te bonds hence leading to nanophase separation. Xu et al.[37] described that upon compression of the crystalline $Ge_1Sb_2Te_4$, Te-Te antisites can be stabilized by the Sb atoms which jump to the vacant

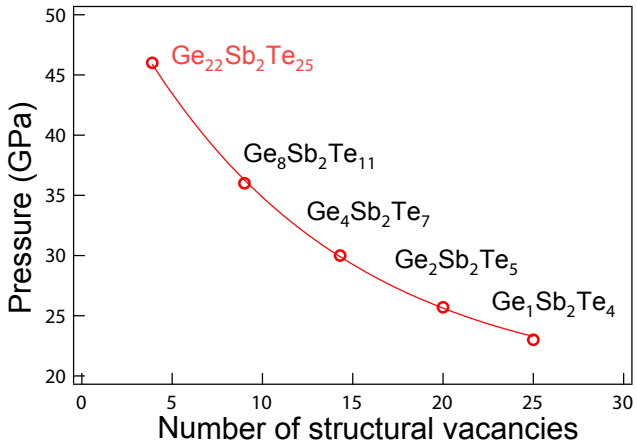

Figure 8: (Color online) Experimentally obtained pressures at 300 K at which total pressure induced amorphization appears in Ge-Sb-Te alloys in dependence on the number of structural vacancies. The predicted $Ge_{22}Sb_2Te_{25}$ composition arises from the exponential fit of experimental pressure values extrapolated to 46 GPa at which GeTe transforms to the BCC phase reported in.[34]

site the Te atoms left behind. They point out that such cooperative antisites Sb and Te hopping is energetically more favourable in contrast to the cooperative antisites Ge and Te hopping. They also emphasized that antisite Sb and Te atoms always appear in pairs and their high concentration can trigger the collapse of the crystalline phase into the amorphous state. Since the $Ge_8Sb_2Te_{11}$ alloy contains 9% of vacancies in the Ge sublattice which is less than half the value for $Ge_2Sb_2Te_5$ (20%), it is speculated that the number of centers, which may destabilize the cubic phase, is insufficient to lead to a large scale nanosegregation process. This may lead to the disordered phase of $Ge_8Sb_2Te_{11}$ containing fewer Te-Te and Sb-Sb(Ge) wrong bonds which can stabilize the amorphous phase.[38] By the analysis of our generated pressure induced amorphous models, we have found that % of Te-Te wrong bonds are 7.2, 8.6, 9.9 and 10.7% for $Ge_8Sb_2Te_{11}$, $Ge_4Sb_2Te_7$, $Ge_2Sb_2Te_5$ and $Ge_1Sb_2Te_4$, respectively and % of Sb-Sb(Ge) antisites are in all compositions similar about 26%. With increasing the Sb content in the Ge-Sb-Te alloys, the number of Te-Te and Sb-Sb(Ge) antisites increases which might support the nanophase separation and thus the stabilization of the amorphous state upon decompression. Vacancy free areas in $Ge_8Sb_2Te_{11}$ may also locally transform from the low to high pressure modifications in a similar way to GeTe or hexagonal $Ge_2Sb_2Te_5$ (crystal to crystal transition) without undergoing nanophase separation[15] and thus

serve to nucleate subsequent recrystallization under decompression.

On the other hand, the presence of the crystalline texture (see Fig. 5 a) may seed recrystallization. It has been demonstrated via molecular dynamic simulations[30] that upon decompression to ambient conditions, the amorphous phase of $Ge_2Sb_2Te_5$ with a crystalline framework existing between 18-22 GPa transforms to the original cubic crystalline structure, whereas an amorphous phase with a trigonal framework (above 22 GPa) converts to another polymorph that is similar to melt-quenched amorphous $Ge_2Sb_2Te_5$. Experimentally, in the range of pressures 18-22 GPa, there is a coexistence of both the amorphous and the crystalline phases in $Ge_2Sb_2Te_5$ with the crystallinity fraction from 0.8 to 0.3.[29] In the case of the low temperature modification of $Ge_8Sb_2Te_{11}$ at 38 GPa, there is only a texture and not a significant crystalline fraction and moreover HT $Ge_8Sb_2Te_{11}$ (see Fig. 5 a) seems to be fully amorphous. Strikingly, both phases revert to the cubic phase at about the same pressure. Therefore while we are not able to exclude the seeding effect in $Ge_8Sb_2Te_{11}$ from the crystalline residue we believe that this contribution is negligible.

The overall results indicate that on one hand the admixture of 14% Sb_2Te_3 in GeTe, the boundary between the existence of the coherently distorted rhombohedral and the stochastically distorted cubic phases at the room temperature, does not block PIA. On the other hand, a Sb_2Te_3 content in GeTe equals of 14% may be the maximum concentration which can trigger spontaneous recrystallization of the PIA phase when decompressed. Therefore $Ge_8Sb_2Te_{11}$ could be considered to be a suitable candidate for reversible crystal to amorphous to crystal cycling under high hydrostatic pressure conditions.

Conclusions

In conclusion, we demonstrated that PIA along the $(GeTe)_x - (Sb_2Te_3)_{1-x}$ tie-line can be observed in both the rhombohedral $Ge_8Sb_2Te_{11}$ and the cubic $Ge_4Sb_2Te_7$ phases as well as below and above the ferroelectric paraelectric transition temperature in $Ge_8Sb_2Te_{11}$. However, we found that the pressure-amorphized $Ge_8Sb_2Te_{11}$ phase begins to revert to the crystalline cubic phase at about

9 GPa in contrast to $Ge_4Sb_2Te_7$ which remains amorphous until ambient conditions when gradually decompressed from 40 GPa. This leads to the conclusion that the concentration of structural vacancies and consequentally increased static disorder in the crystalline phases containing higher than 14% Sb_2Te_3 may play a crucial role in the degradation of memory via an increased nanophase separation in pressure-amorphized Ge-Sb-Te alloys. Moreover, experimentally, we observed that pressure induced amorphization in $Ge_8Sb_2Te_{11}$ is thermally activated. The onset of amorphization is at about 25.2 GPa and 27.5 GPa for 405 K and 300 K, respectively and the material completely amorphizes at 32 GPa at 405 K while crystalline texture can be seen until 38 GPa (the last measure point) at 300 K. In order to verify the thermal contribution to PIA we performed DFT calculations along the $(GeTe)_x - (Sb_2Te_3)_{1-x}$ tie-line under large hydrostatic pressure. First, we found that in silico models of $Ge_2Sb_2Te_5$ and $Ge_8Sb_2Te_{11}$ became totally amorphous at the same pressure points as experiment at 300 K and 400 K. Second, we calculated the pressure-temperature dependences of PIA for $Ge_1Sb_2Te_4$, $Ge_2Sb_2Te_5$ and $Ge_8Sb_2Te_{11}$ which were exponential in all cases. However, we showed that $Ge_8Sb_2Te_{11}$ will not convert to the amorphous phase until 100 GPa at 1 K, a value about 15 GPa higher than the predicted value from the pressure-temperature plot.

Acknowledgement

Measurements were performed at the ESRF at beamline ID09A within the HS3510 proposal. The authors acknowledge Projects No. LM2015082 and CZ.1.05/4.1.00/11.0251 Center of Materials and Nanotechnologies cofinanced by the European Fund of the Regional Development and the state budget of the Czech Republic.

References

(1) Yamada, N.; Ohno, E.; Nishiuchi, K.; Akahira, N.; Takao, M.Rapid Phase-Transitions of $(GeTe)_x - (Sb_2Te_3)_{1-x}$ pseudobinary amorphous thin-films for an optical disk memory. *J. Appl. Phys.* **1991**, *69*, 2849–2856.

(2) Wuttig, M.; Yamada, N.Phase-change materials for rewriteable data storage. *Nature Mater.* **2007**, *6*, 824–832.

(3) Loke, D.; Lee, T. H.; Wang, W. J.; Shi, L. P.; Zhao, R.; Yeo, Y. C.; Chong, T. C.; Elliott, S. R. Breaking the Speed Limits of Phase-Change Memory. *Science* **2012**, *336*, 1566–1569.

(4) Kwon, J. B. Exploiting Storage Class Memory for Future Computer Systems: A Review. *IETE Technical Review* **2015**, *32*, 218–226.

(5) Nukala, P.; Lin, C.-C.; Composto, R.; Agarwal, R. Ultralow-power switching via defect engineering in germanium telluride phase-change memory devices. *Nat. Commun.* **2016**, *7*, 10482.

(6) Kallika, J.; Akola, J.; Jones, R. O. Crystallization processes in the phase change material $Ge_2Sb_2Te_5$: Unbiased density functional/molecular dynamics simulations. *Phys. Rev. B* **2016**, *94*, 134105.

(7) Simpson, R. E.; Krbal, M.; Fons, P.; Kolobov, A. V.; Tominaga, J.; Uruga, T.; Tanida, H. Toward the Ultimate Limit of Phase Change in $Ge_2Sb_2Te_5$. *Nano. Lett* **2010**, *10*, 414–419.

(8) Kalikka, J.; Zhou, X.; Dilcher, E.; Wall, S.; Li, J.; Simpson, R. E. Strain engineered diffusive atomic switching in two-dimensional crystals.*Nat. Commun.* **2016**, *7*, 11983.

(9) Zhou, X.; Kalikka, J.; Ji, X.; Wu, L.;Song, Z.; Simpson, R. E. Phase change memory materials by design: a strain engineering approach.*Adv. Mater.* **2016**, *28*, 3007–3016.

(10) Eising, G.; Puza, A.; Kooi, B. J. Stress-Induced Crystallization of Ge-Doped Sb Phase-Change Thin Films. *Cryst. Growth Des.* **2013**, *13*, 220–225.

(11) Xu, M.; Y. Q. Cheng and, L. W.; Sheng, H. W.; Meng, Y.; Yang, W. G.; Han, X. D.; Ma, E. Pressure tunes electrical resistivity by four orders of magnitude in amorphous $Ge_2Sb_2Te_5$ phase-change memory alloy. *PNAS* **2012**, *109*, 1055–1062.

(12) Nakamura, Y.; Numata, M.; Hoshino, H.; Shimoji, M. Electrical conductivity of Ge-Te glasses under hydrostatic pressure. *J. Non-Cryst. Solids* **1975**, *17*, 259–265.

(13) Liu, J. A multi-scale analysis of the impact of pressure on melting of crystalline phase change material germanium telluride. *Appl. Phys. Lett.* **2014**, *105*, 173509.

(14) Kolobov, A. V.; Haines, J.; Pradel, A.; Ribes, M.; Fons, P.; Tominaga, J.; Katayama, Y.; Hammouda, T.; Uruga, T. Pressure-Induced Site-Selective Disordering of $Ge_2Sb_2Te_5$: A New Insight into Phase-Change Optical Recording. *Phys. Rev. Lett.* **2006**, *97*, 035701.

(15) Krbal, M.; Kolobov, A. V.; Haines, J.; Fons, P.; Levelut, C.; Le Parc, R.; Hanfland, M.; Tominaga, J.; Pradel, A.; Ribes, M. Initial Structure Memory of Pressure-Induced Changes in the Phase-Change Memory Alloy $Ge_2Sb_2Te_5$. *Phys. Rev. Lett.* **2009**, *103*, 115502.

(16) Hsieh, W.-P.; Zalden, P.; Wuttig, M.; Lindenberg, A. M.; Mao, W. L. High-pressure Raman spectroscopy of phase change materials. *Appl. Phys. Lett.* **2013**, *103*, 191908.

(17) Onodera, A.; Sakamoto, I.; Fujii, Y.; Mori, N.; Sugai, S. Structural and electrical properties of GeSe and GeTe at high pressure. *Phys. Rev. B* **1997**, *56*, 7935–7941.

(18) Sun, Z.; Zhou, J.; Mao, H.-K.; Ahuja, R. Peierls distortion mediated reversible phase transition in GeTe under pressure. *PNAS* **2012**, *109*, 5948–5952.

(19) Zhao, J.; H. Liu, L. E.; Chen, Z.; Sinogeikin, S.; Zhao, Y.; Gu, G. Pressure-Induced Disordered Substitution Alloy in Sb_2Te_3 . *Inorg. Chem.* **2011**, *50*, 11291–11293.

(20) Krbal, M.; Kolobov, A. V.; Fons, P.; Haines, J.; Pradel, A.; Ribes, M.; Piarristeguy, A. A.; Levelut, C.; Le Parc, R.; Agafonov, V.; Hanfland, M.; Tominaga, J. Pressure-induced struc-

tural transitions in phase-change materials based on Ge-free Sb-Te alloys. *Phys. Rev. B* **2011**, *83*, 024105.

(21) Matsunaga, T.; Morita, H.; Kojima, R.; Yamada, N.; Kifune, K.; Kubota, Y.; Tabata, Y.; Kim, J.-J.; Kobata, M.; Ikenaga, E.; Kobayashi, K. Structural characteristics of GeTe-rich GeTe-Sb_2Te_3 pseudobinary metastable crystals. *J. Appl. Phys.* **2008**, *103*, 093511.

(22) Fons, P.; Kolobov, A. V.; Krbal, M.; Tominaga, J.;Andrikopoulos, K. S.;Yannopoulos, S. N.; Voyiatzis, G. A.; Uruga, T. Phase transition in crystalline GeTe: Pitfalls of averaging effects *Phys. Rev. B* **2010**, *82*, 155209.

(23) Krbal, M.; Kolobov, A. V.; Fons, P.; Simpson, R. E.; Matsunaga, T.; Tominaga, J.; Yamada, N. Local atomic order of crystalline $Ge_8Sb_2Te_{11}$ across the ferroelectric to paraelectric transition: The role of vacancies and static disorder. *Phys. Rev. B* **2011**, *84*, 104106.

(24) Caravati, S.; Bernasconi, M.; K00FChne, T. D.; Krack, M.; Parrinello, M. Unravelling the mechanism of pressure induced amorphization of phase change materials. *Phys. Rev. Lett.* **2009**, *102*, 205502.

(25) Edwards, A. H.; Pineda, A. C.; Schultz, P. A.; Martin, M. G.; Thompson, A. P.; Hjalmarson, H. P. Theory of persistent, p-type, metallic conduction in c-GeTe. *J. Phys.: Condens. Matter.* **2005**, *18*, 329–335.

(26) Segall, M.; Lindan, P. J. D.; Probert, M.; Pickard, C.; Hasnip, P.; Clark, S.; Payne, M. First-principles simulation: ideas, illustrations and the CASTEP code.*J. Phys. Condens. Matter* **2002**, *24*, 2717–2744.

(27) Ceperley, D. M.; Alder, B. J. Ground State of the Electron Gas by a Stochastic Method. *Phys. Rev. Lett.* **1980**, *45*, 566–569.

(28) Perdew, J. P.; Zunger, A. Self-interaction correction to density-functional approximations for many-electron systems. *Phys. Rev. B* **1981**, *23*, 5048–5079.

(29) Krbal, M.; Kolobov, A. V.; Haines, J.; Fons, P.; Levelut, C.; Le Parc, R.; Hanfland, M.; Tominaga, J.; Pradel, A.; Ribes, M. Temperature independence of Pressure-Induced amorphization of the Phase-Change Memory Alloy $Ge_2Sb_2Te_5$. *Appl. Phys. Lett.* **2008**, *93*, 031918.

(30) Sun, Z.; Zhou, J.; Pan, Y.; Song, Z.; Mao, H.-K.; Ahuja, R. Pressure-induced reversible amorphization and an amorphous - amorphous transition in $Ge_2Sb_2Te_5$ phase-change memory material. *PNAS* **2011**, *108*, 10410–10414.

(31) Bustingorry, S.; Jagla, E. A. Mechanical versus thermodynamical melting in pressure-induced amorphization:The role of defects. *Phys. Rev. B* **2004**, *69*, 064110.

(32) Nonaka, T.; Ohbayashi, G.; Toriumi, Y.; Mori, Y.; Hashimoto, H. Crystal structure of GeTe and $Ge_2Sb_2Te_5$ meta-stable phase *Thin Solid Films* **2000**, *370*, 258-261.

(33) Krbal, M.; Kolobov, A.; Fons, P.; Tominaga, J.; Elliott, S.; Guissani, A.; Perumal, R., K.and Calarco; Matsunaga, T.; Yamada, N.; Nitta, K.; Uruga, T. Crystalline GeTe-based phase-change alloys: Disorder in order. *Phys.Rev.B* **2012**, *86*, 045212.

(34) Kabalkina, S. S.; Vereshchagin, L. F.; Serebryanaya, N. R. Phase Transition in Germanium Telluride at High Pressures. *Sov. Phys.-JETP* **1967**, *24*, 917–919.

(35) Yang, Y. L. Structural and electronic properties of GeTe under pressure: ab initio study. *Materials Technology* **2013**, *28*, 305-309.

(36) Arora, A. K. Pressure-induced amorphization versus decomposition. *Solid State Commun.* **2000**, *115*, 665–668.

(37) Xu, M.; Zhang, W.; Mazzarello, R.; Wuttig, M. Disorder Control in Crystalline $GeSb_2Te_4$ Using High Pressure. *Adv. Sci.* **2015**, *2*, 1500117.

(38) Deringer, V. L.; Zhang, W.; Lumeij, M.; Maintz, S.; Wuttig, M.; Mazzarello, R.; Dronskowski, R. Bonding Nature of Local Structural Motifs in Amorphous GeTe. *Angewandte Chemie, International Edition* **2014**, *53*, 10817–10820.

For Table of Contents Only

The pressure induced phase transition in both coherently distorted rhombohedral $Ge_8Sb_2Te_{11}$ and randomly distorted cubic $Ge_4Sb_2Te_7$ phases is presented. While coherent distortion in $Ge_8Sb_2Te_{11}$ does not prevent the amorphization event in a similar manner as pure GeTe, the pressure-amorphized $Ge_8Sb_2Te_{11}$ phase begins to revert to the crystalline cubic phase at about 9 GPa in contrast to $Ge_4Sb_2Te_7$ which remains amorphous at ambient conditions. Roles of a vacancy concentration in Ge-Sb-Te and temperature are shown.